The cohesin ring concatenates sister DNAs

Christian H. Haering[1,2,4], Ana-Maria Farcas[1,4], Prakash Arumugam[1,3], Jean Metson[1] & Kim Nasmyth[1]

[1]University of Oxford, Department of Biochemistry, South Parks Road, Oxford, OX1 3QU, UK. [2]Present address: European Molecular Biology Laboratory (EMBL), Meyerhofstraße 1, 69117 Heidelberg, Germany. [3]Present address: Department of Biological Sciences, University of Warwick, Gibbet Hill Road, Coventry, CV4 7AL, UK. [4]These authors contributed equally to this work.

This is the unedited version of the manuscript published in final form in Nature Vol. 454: 297-301, online at http://www.nature.com/nature/journal/v454/n7202/abs/nature07098.html

Corresponding author: Kim Nasmyth, University of Oxford, Department of Biochemistry, South Parks Road, Oxford, OX1 3QU, UK; kim.nasmyth@bioch.ox.ac.uk

Summary

Sister chromatid cohesion, which is essential for mitosis, is mediated by a multi-subunit protein complex called cohesin whose Scc1, Smc1, and Smc3 subunits form a tripartite ring structure. It has been proposed that cohesin holds sister DNAs together by trapping them inside its ring. To test this, we used site-specific cross-linking to create chemical connections at the three interfaces between the ring's three constituent polypeptides, thereby creating covalently closed cohesin rings. As predicted by the ring entrapment model, this procedure produces dimeric DNA/cohesin structures that are resistant to protein denaturation. We conclude that cohesin rings concatenate individual sister minichromosome DNAs.

Introduction

Sister chromatid cohesion is mediated by a multi-subunit complex called cohesin that contains four core subunits: Smc1 and Smc3, members of the SMC (Structural Maintenance of Chromosomes) protein family, and two non-SMC subunits, Scc1/Mcd1, a member of the kleisin family, and Scc3/SA [1,2]. Sister chromatid disjunction occurs when all chromosomes have been bi-oriented and is triggered by site-specific cleavage of cohesin's Scc1 subunit by separase [3]. Cohesin's Smc1 and Smc3 both form rod shaped molecules that heterodimerize via "hinge" domains situated at the ends of 30 nm long intra-molecular antiparallel coiled coils [4,5]. ATPase "heads" at the other ends are connected by cohesin's Scc1 kleisin subunit, thereby forming a tripartite ring with a 35 nm diameter [4,6]. It has been proposed that cohesin holds sister chromatids together by trapping sister DNAs inside its ring. By severing Scc1, separase is envisioned to open the ring and thereby release sister DNAs from their topological embrace.

To investigate the physical nature of sister chromatid cohesion, we have recently used sucrose gradient sedimentation and gel electrophoresis to purify from yeast cohesed sister chromatids of small circular minichromosomes [7]. The minichromosome dimers are composed of individual DNAs packaged into nucleosomes that are converted to monomers by cleaving Scc1 or by linearizing their DNA. Importantly, their formation depends on centromeres as well as cohesin (see Supplementary Information and Fig. S1). These data are consistent with (but do not prove) the notion that cohesin attaches to chromatin using a topological mechanism. However, they do not exclude the possibility that cohesion requires the non-topological association of cohesin rings bound to different chromatin fibres [8]. If cohesin holds dimeric minichromosomes together by trapping them inside its ring, then introducing covalent connections between the Smc1/Smc3 hinge, Smc1 head/Scc1-C and Smc3 head/Scc1-N interfaces should create a chemically circularized cohesin ring within which sister DNAs would be trapped even after protein denaturation (Fig. 1a). We describe here experiments that test this crucial prediction.

Covalent connection of the three cohesin ring subunits

To connect cohesin subunit interfaces covalently, we used the homobifunctional thiol-reactive chemicals dibromobimane (bBBr) and bis-maleimidoethane (BMOE) that bridge thiol groups up to 5 Å or 8 Å respectively [9,10] (Supplementary Fig. S2). We created a homology model [11] of the yeast Smc1/Smc3 hinge heterodimer based on the homodimeric *Thermotoga maritima* crystal structure [4] and identified two juxtaposed side-chains that we mutated to cysteines. Incubation of the engineered Smc1/Smc3 hinge dimer with either bBBr or BMOE caused efficient cross-linking within a few minutes (Fig. 1b). Crucially, cross-linking was dependent on both cysteine substitutions. We used the same approach to connect the loop between the two ß-strands of Scc1's winged-helix to a ß-strand in Smc1's ATPase head [12] (Fig. 1c). Because no structural information is available for the interface between Smc3's ATPase and Scc1's N-terminal domain, we expressed Smc3 and Scc1 as a fusion protein, using a long flexible linker containing triple target sequences for the TEV protease to connect Smc3's C-terminus with Scc1's N-terminus (Smc3-TEV-Scc1) [13]. To create cohesin rings that could be chemically circularized

by BMOE or bBBr, the cysteine substitutions were introduced into Smc3-TEV-Scc1 and Smc1.

Cohesin circularization produces SDS resistant minichromosome dimers

A 2.3 kbp circular minichromosome [7] was introduced into yeast strains whose Smc1 and Smc3-TEV-Scc1 polypeptides contained either all four cysteine substitutions or only a subset of these. After nocodazole arrest and cell lysis, extracts were centrifuged through sucrose gradients and fractions containing monomeric and dimeric minichromosomes detected by native agarose gel electrophoresis and Southern blotting. Importantly, dimeric minichromosomes could still be isolated from yeast cells whose cohesin ring subunits had been engineered to permit cohesin circularization. The cysteine substitutions had little adverse effect, but the fusion of Scc1 to Smc3 roughly halved the fraction of dimeric minichromosomes (Fig. 2a). This was not surprising as the fusion causes partial cohesion defects *in vivo* [13]. DTT, sucrose and other low molecular weight contaminants were removed from the gradient fractions by dialysis and cohesin subunits treated with bBBr, BMOE, or merely DMSO solvent. After quenching the reaction by re-addition of DTT, SDS was added to a finalconcentration of 1% and the samples were heated to 65°C for four minutes. The denatured samples were finally electrophoresed in agarose gels containing ethidium bromide and minichromosome DNA was detected by Southern blotting.

Dimer fractions from control cells expressing unmodified cohesin contained four species of DNA (Fig. 2b, panel F). The fastest migrating and most predominant are supercoiled monomers (①). Due to SDS in the loading buffer, the next two species (② and ③) were poorly resolved from each other. These DNAs co-migrated with monomeric nicked circles produced by nicking enzyme after removal of nucleosomes with 2 M KCl (Fig. 2d) and with (infrequently) intertwined (i.e. concatenated) supercoiled DNAs isolated from a topoisomerase II mutant (Fig. 2e) and therefore include both of these species of DNA. The nicking enzyme treatment revealed that about 10% of DNAs from dimer (but not monomer) fractions are DNA-DNA concatemers (Fig. 2d and data not shown). The least abundant species (④) migrated more slowly than two intertwined supercoiled circles (③) but more rapidly than two intertwined nicked circles generated by treatment with nicking enzyme (⑤). We conclude that these DNAs correspond to one supercoiled circle intertwined with one nicked circle.

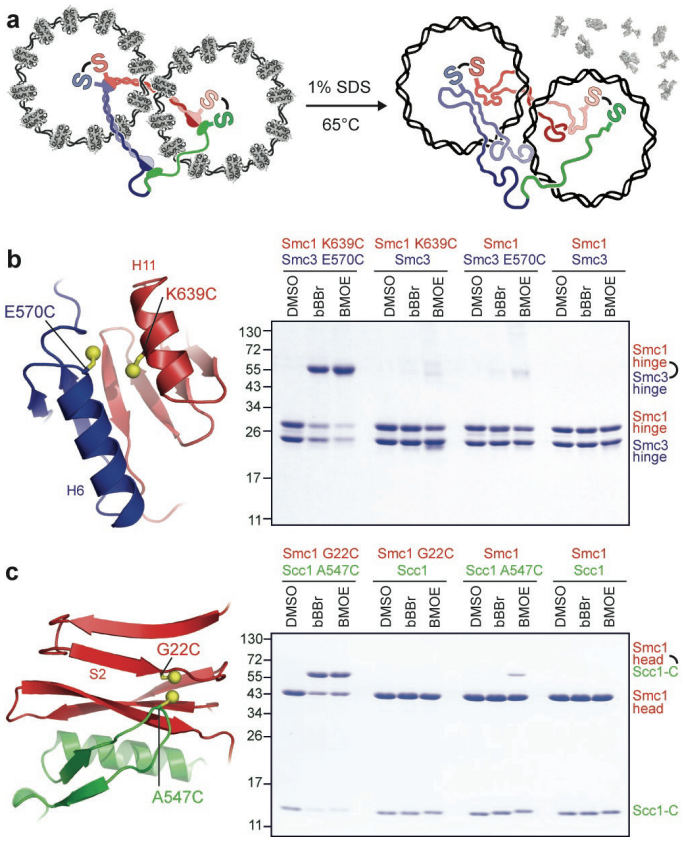

Treatment of dimer fractions with bBBr or BMOE had no effect on the electrophoresis profile of minichromosome DNAs (Fig. 2b, F). Moreover, the very same pattern was observed when dimeric minichromosomes were isolated from strains expressing the Smc3-TEV-Scc1 fusion (Fig. 2b, E) and cross-linkable cysteine pairs at either the Smc1/Scc1 or the Smc1/Smc3 interface (Fig. 2b, C and D). In contrast, bBBr and BMOE but not DMSO alone caused the appearance of two additional species of DNA when dimers were isolated from a strain containing the Smc3-TEV-Scc1 fusion and cysteine pairs at both interfaces (Fig. 2b, B). The more abundant (⑦) migrated slightly more slowly than intertwined supercoiled circles whereas the less abundant (⑧) migrated slightly more slowly than supercoiled circles intertwined with nicked circles. Their electrophoretic mobilities and the fact that neither was detected when identical cross-linking reactions were conducted with monomer fractions (Fig. 2b, A) suggest that they represent novel dimeric forms. Their formation occurs at the expense of supercoiled and nicked monomeric circles.

Our data suggest that the faster form (⑦) is a dimer of supercoiled monomeric circles associated with cohesin while the slower form (⑧) is a dimer between supercoiled and nicked circles associated with cohesin. Consistent with this, both were converted to a form (⑨) that

Figure 1. Making covalently closed cohesin rings. a Experimental strategy: fusion of the Smc3 C-terminus with the Scc1 N-terminus and chemical cross-linking of engineered cysteine residues at the Smc1/Smc3 and Smc1/Scc1 interfaces creates a covalently closed cohesin ring. Circular sister DNAs should remain cohesed even after protein denaturation if and only if they are trapped inside cohesin's ring. **b** A homology model of the Smc1/Smc3 hinge interface to the homodimeric bacterial structure (PDB 1GXL) identifies two juxtaposed Cβ atoms in Smc1's helix H11 and Smc3's helix H6 at a distance compatible with cross-linking when mutated to cysteine. Wild-type and cysteine mutant yeast Smc1/Smc3 hinge domain dimers were incubated with DMSO, bBBr, or BMOE, denatured and run on SDS-PAGE followed by Coomassie Blue staining. **c** The structure of the yeast Scc1 C-terminus bound to Smc1's head domain (PDB 1W1W) identifies two juxtaposed side-chains that should allow cross-linking when mutated to cysteine. Purified complexes of wild-type and cysteine mutant yeast Smc1 head domain bound to Scc1's C-terminal domain were incubated with DMSO, bBBr, or BMOE, denatured and run on SDS-PAGE followed by Coomassie Blue staining. The low level crosslinking observed for the Smc1/Scc1(A547C) combination likely results from a reaction of BMOE with the engineered cysteine in Scc1 and the nearby ε-amino group of Smc1's lysine residue K20.

co-migrates with intertwined nicked circles (⑤) when treated with nicking enzyme (Fig. 2d). The extra mass of cohesin probably has little effect on the electrophoretic mobility of this slow running species. Importantly, neither novel dimer was produced when just one of the four cysteine substitutions was lacking (Supplementary Fig. S3a), implying that they arise due to the simultaneous cross-linking of both cysteine pairs at the Smc1/Smc3 hinge and Smc1/Scc1 interfaces. Cross-linked dimers were also produced when minichromosomes were isolated from cycling cultures (Supplementary Fig. S3a), suggesting that their formation is not an artefact caused by arresting cells with nocodazole. Finally, no slower migrating species could be observed when DNA was linearized with a restriction enzyme after cross-linking (Supplementary Fig. S3b). In conclusion, covalent closure of the cohesin ring converts dimeric but not monomeric minichromosomes to a dimeric form that is resistant both to SDS and to 2 M KCl (native dimers are converted to monomers at 0.5-1 M KCl; Supplementary Fig. S4).

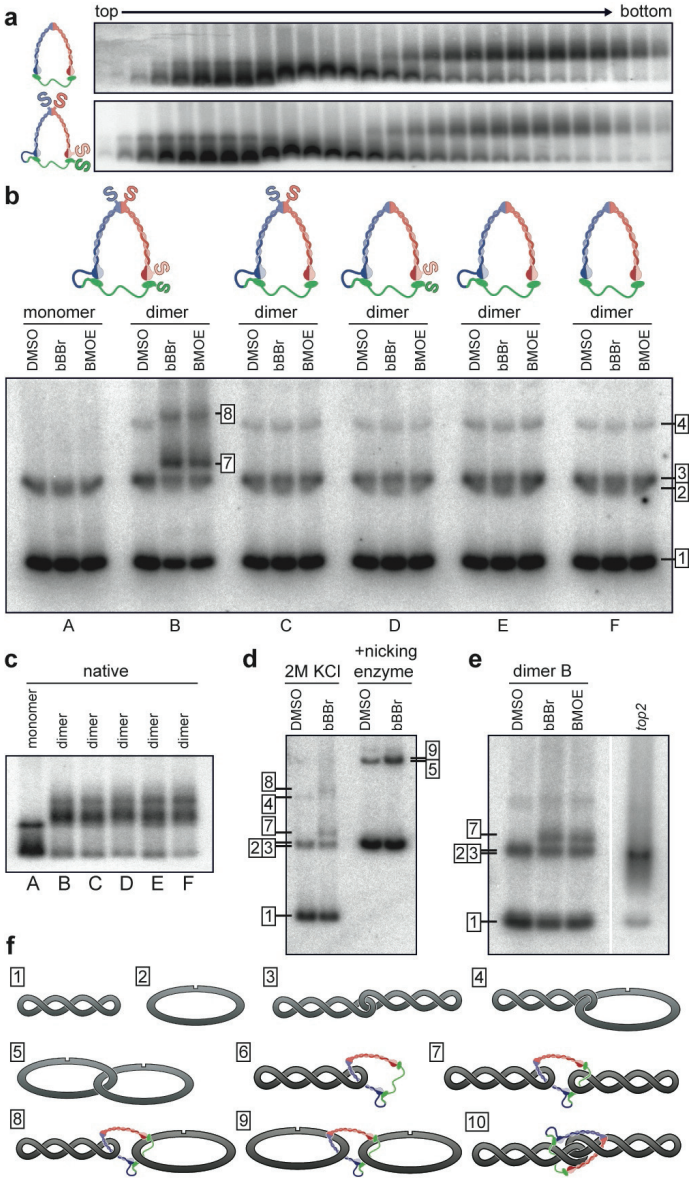

Figure 2. Covalent cohesin circularization creates SDS-resistant minichromosome DNA dimers. a Extracts from yeast strains harbouring the minichromosome and expressing wild-type cohesin (top) or Smc3-TEV-Scc1 and Smc1 containing the engineered cysteine pairs (bottom) were separated by gradient centrifugation followed by native gel electrophoresis and Southern blotting. Minichromosome dimers sediment faster but electrophorese slower than monomers. The fraction of dimers is reduced by the Smc3-TEV-Scc1 fusion. **b** Monomer or dimer gradient fractions from yeast strains in which all three (K14856; panels A and B), only two (K14857, K14859; C and D), one (K14858; E), or no (K14860; F) ring subunit interface(s) can be covalently linked were treated with DMSO, bBBr, or BMOE before protein denaturation, electrophoresis and minichromosome DNA detection by Southern blotting. Monomer and dimer fractions contain supercoiled (①) and nicked (②) monomeric minichromosomes. Dimer fractions also contain supercoiled-supercoiled (③) and supercoiled-nicked (④) concatenated minichromosome DNAs. Only samples in which all three cohesin ring subunit interfaces have been covalently linked contain additional slower migrating bands, presumably corresponding to supercoiled-supercoiled (⑦) and supercoiled-nicked (⑧) cohesed minichromosomes. **c** Input fractions for cross-linking reactions A-F were run without denaturation on an agarose gel and Southern blotted. **d** Treatment of non-cross-linked or cross-linked minichromosomes with nicking enzyme after removal of nucleosomes by high salt converts supercoiled (①), supercoiled-supercoiled (③, ⑦) or supercoiled-nicked (④, ⑧) minichromosomes to nicked (②) or nicked-nicked (⑤, ⑨) forms. **e** Gradient dimer fractions from a topoisomerase II mutant strain (K15029) grown at the restrictive temperature were denatured with SDS. Concatenated minichromosomes (short exposure) co-migrate with bands ② and ③ of K14856 (long exposure) on the same agarose gel. **f** Schemata of minichromosome conformations.

Circularized cohesin holds individual DNAs together

To test whether the SDS-resistant dimers produced by cohesin circularization are indeed monomeric DNAs held together by cohesin, we employed two-dimensional (2D) gel electrophoresis. Denatured cross-linked samples were resolved on an agarose gel as before (the first dimension) and then electrophoresed perpendicularly through a thin zone of agarose or agarose containing proteinase K into a second agarose gel (the second dimension). Proteinase K should digest any proteins before DNAs enter the second gel and DNAs that ran as dimers in the first dimension should run as monomers in the second dimension if they were initially held together by a proteinaceous (i.e. cohesin) connection. In the absence of proteinase K, all DNA species migrate identically in first and second dimensions and therefore lie on a diagonal line (Fig. 3a). Several species also ran on the diagonal in the presence of proteinase K, namely monomeric supercoils (①), monomeric nicked circles (②), intertwined supercoils (③), and nicked circles intertwined with supercoils (④) (Fig. 3a). In contrast, DNAs of presumptive dimers of two supercoiled minichromosomes held together by cohesin (⑦) migrated as monomeric supercoils in the second dimension (⑦→①), while presumptive supercoiled-nicked circle dimers held together by cohesin (⑧) split into monomeric supercoils (⑧→①) and nicked circles (⑧→②). We conclude that chemical circularization of cohesin associated with native dimeric minichromosomes is accompanied by the cross-linking of monomeric DNAs to create SDS-resistant but protease sensitive dimers.

The protease containing 2D gel revealed two new types of low abundance DNAs. The first (⑥) migrated considerably slower than monomeric supercoils in the first dimension but ran as monomeric supercoils in the second dimension (⑥→①). These DNAs were only detected in monomeric or dimeric minichromosome preparations in which cohesin rings had been covalently closed (data not shown). They presumably correspond to rare supercoiled monomers whose migration is retarded by their association with (entrapment by) a chemically circularized cohesin ring. The second species (⑩) co-migrated with cohesin-mediated supercoiled dimers in the first

dimension but with intertwined supercoils (and nicked circles) in the second dimension. These DNAs could correspond either to

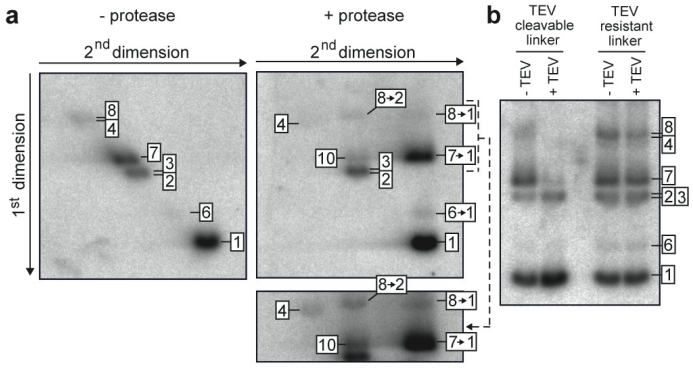

Figure 3. Cohesin's covalent circularization holds individual DNAs together. a Cross-linked and denatured samples were run on an agarose gel, lanes cut out, and run on a second agarose gel in perpendicular direction. A thin slot between the first dimension lane and the second gel was filled with either agarose or agarose containing 0.2 mg/ml proteinase K. In the absence of protease, all bands run on a diagonal. In the presence of protease, supercoiled-supercoiled cohesed dimers (⑦) run as supercoiled monomers (⑦→①) in the second dimension, while supercoiled-nicked cohesed dimers (⑧) split up into supercoiled (⑧→①) and nicked (⑧→②) monomers in the second dimension, more clearly visible in a longer exposure (panel below). A faint band presumably corresponding to cohesin bound supercoiled monomers (⑥) is converted into naked supercoiled monomers (⑥→①) upon protease cleavage. An additional band (⑩) running off the diagonal presumably corresponds to supercoiled-supercoiled concatenated minichromosomes that had bound cohesin. **b** Cross-linked minichromosome samples were treated with or without TEV protease before SDS protein denaturation, agarose gel electrophoresis and Southern blotting. The slower migrating bands (⑦, ⑧) corresponding to cohesed minichromosomes disappear upon TEV incubation if the Smc3-Scc1 linker contains triple target sequences for the protease (TEV cleavable), but not if the -1 sites of the triple target sequence have been mutated to lysine (TEV resistant).

monomeric nicked circles associated with cohesin or, more likely, to intertwined supercoils that are also associated with cohesin.

If cohesin circularization by bBBr and BMOE cross-linking per se is responsible for the formation of SDS-resistant minichromosome dimers, then cleavage of the cohesin ring should be sufficient to release the monomeric DNAs. To test this, we incubated cross-linked dimeric minichromosome preparations with or without TEV protease to cleave the linker connecting Smc3 and Scc1. The presence of TEV greatly reduced both types of DNA dimers induced by cohesin's circularization (⑦ and ⑧), which was accompanied by a corresponding increase in monomeric DNAs (① and ②) (Fig. 3b). This effect was clearly caused by cleavage of the TEV sites in the Smc3-Scc1 linker because DNA dimers produced by circularization of cohesin with a TEV-resistant Smc3-Scc1 linker were unaffected by TEV protease (Fig. 3b). We conclude that the SDS-resistant association of sister DNAs induced by cross-linking cohesin's three subunits does not merely accompany the circularization of cohesin but actually depends on it.

Are minichromosomes held together by single or double cohesin rings?

The simplest explanation for the cross-linking results is that sister DNAs are topologically trapped within single (monomeric) cohesin rings (Supplementary Fig. S5a). An alternative albeit more complicated possibility envisions entrapment of sister DNAs by rings that are themselves topologically intertwined (Supplementary Fig. S5b) or by dimeric cohesin rings. Only two cysteine cross-links are needed for entrapment by single rings, while four are required by double ring models. If we knew the efficiency with which bBBr and BMOE cross-link the Smc1/Smc3 and Smc1/Scc1 interfaces and the number of cohesin bridges, then we could calculate the fraction of DNAs that should be trapped as dimers according to the two models and compare these to what is actually observed. To estimate the protein cross-linking efficiency, we spiked cross-linkable minichromosome dimer preparations with purified Smc1/Smc3 hinge or Smc1 head/Scc1-C before cross-linking with bBBr or PAGE and the fraction of proteins cross-linked measured after SYPRO ruby staining (Fig. 4a). The other half was run on an agarose gel and the fraction of DNAs dimerized measured by Southern blotting (Fig. 4b). The fraction of rings expected to be cross-linked at

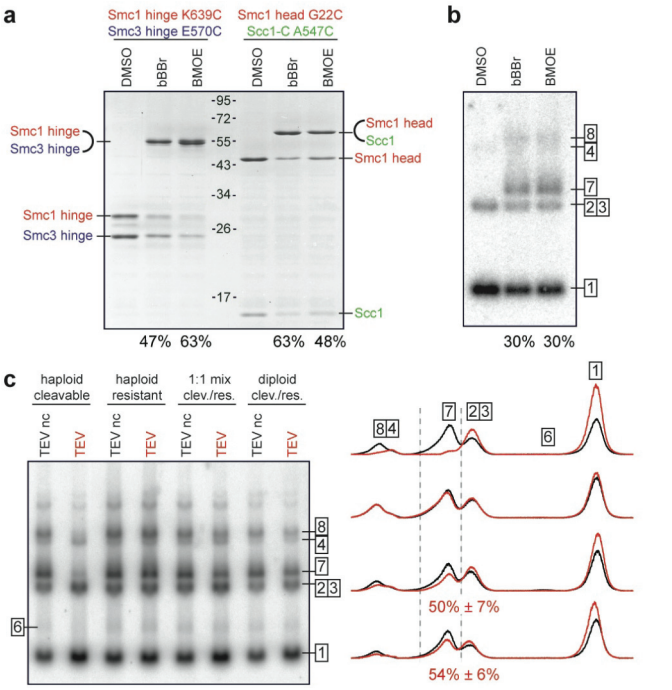

Figure 4. Minichromosomes are cohesed by single cohesin rings. a Protein-protein cross-linking efficiencies by bBBr and BMOE were measured by spiking dimer fractions (K14856) with purified double cysteine mutants of Smc1/Smc3 hinge or Smc1/Scc1-C complex preparations. After cross-linking, half of the reactions were run on an SDS-PAGE and band intensities were measured after SYPRO Ruby staining. **b** The other half of the reactions were run on an agarose gel and the fractions of cohesed minichromosomes (⑦+⑧/total) were quantified after Southern blotting. **c** Minichromosome dimer fractions from haploid strains expressing Smc3-Scc1 fusions containing TEV target sequences (K14856) or resistant to TEV cleavage (K15089), from a 1:1 mixture of the two haploid strains, or from a diploid strain containing one TEV cleavable and one TEV resistant *SMC3-SCC1* allele (K15267) were cross-linked with bBBr, treated with wild-type or a non-catalytic (nc; C151A) mutant of TEV protease, denatured, run on an agarose gel and Southern blotted. Lane profiles were recorded, the peaks corresponding to cohesed supercoiled minichromosome dimers (⑦) integrated and the peak area after incubation with active versus non-catalytic TEV protease compared. In case the number of cohesin cross-bridges follows a Poisson distribution, we would expect 53% or 27% of cross-linked dimers surviving TEV treatment for single or double ring models, respectively. The observed value is 54% ± 6% (mean of three independent experiments ± standard deviation).

both interfaces, which is given by multiplying individual cross-linking efficiencies, was 30% for both bBBr and BMOE. We would therefore expect 30% of DNAs to be dimerized if held together by a single cohesin ring but only 9% by a double ring. Estimating the actual number of bridges is harder because the gradient fractions contain much cohesin not associated with minichromosomes (data not shown). However, if we assume that a single bridge is sufficient to hold sister DNAs together and that cross-bridges form *in vivo* and survive fractionation *in vitro* with a defined probability (λ), then the fraction of chromosomes *f(x)* with *0, 1, 2, ... n* bridges should fit a Poisson distribution. *f(0)* can be measured directly, namely by measuring the fraction of monomeric minichromosomes (Supplementary Fig. S6a) and DNA-DNA concatemers (Fig. 2d), which permits calculation of λ (see Supplementary Information). Because *f(0)* is large, most native dimeric minichromosomes are predicted to have a single bridge. Taking this into account, the single and double ring models predict 32% and 10% dimerization, respectively. The observed value with both reagents was 30% (Fig. 4b), which is inconsistent with the double ring model and close to that predicted by the single ring model.

Single and double ring models also make different predictions for heterozygous diploids that express equal amounts of TEV-cleavable and TEV-resistant Smc3-Scc1 fusion proteins (Supplementary Fig. S6b). In the case of one cross-bridge, the single ring model predicts that 50% of cross-linked dimers should survive cleavage of half the cohesin rings. In contrast the double ring model predicts only 25% because cleavage of just one ring is sufficient to destroy dimers held together by intertwined rings. We isolated minichromosome dimers from cleavable and non-cleavable haploids, a 1:1 mixture of the two, and from heterozygous diploids. These were cross-linked, treated either with TEV protease or a non-catalytic TEV mutant, denatured with SDS and run on an agarose gel. The fraction of DNAs dimerized by cross-linking was measured by scanning Southern blots. This revealed that about 50% of cohesed minichromosomes survived TEV treatment when isolated from heterozygous diploids as well as the 1:1 mixture of haploids (Fig. 4c). These data fit the single but not the double ring model. We note that the latter also predicts that a sizeable fraction of cross-linked dimers (⑦ and ⑧) from heterozygous diploids should be converted by TEV cleavage to supercoiled monomers associated with cohesin (⑥), which is not observed (Fig. 4c).

Discussion

Our cross-linking experiments are consistent with the notion that sister minichromosome DNAs are entrapped by a single monomeric ring. Importantly, they exclude the possibility that the connection between sister DNAs is mediated by non-topological interactions between cohesin complexes associated with each sister [8]. Given the specificity of the cross-linking by bBBr and BMOE, there is no reason to suppose that putative interactions between cohesin rings will have been cross-linked in our experiments. Double ring models envisioning topological cohesin-cohesin interactions or a gigantic ring formed by two cohesin complexes are difficult to reconcile with the findings that the fraction of DNAs dimerized is almost identical to the fraction of cohesin rings circularized and not to the square of this fraction and that cleavage of half the cohesin rings reduces dimers to 50% and not 25%.

Our conclusion that sister chromatin fibres of dimeric minichromosomes are threaded through cohesin rings provides a simple and potentially adequate mechanism to explain cohesin's ability to hold sister chromatids together. Cohesin could therefore be considered a "concatenase". It will be important to address whether it uses the same mechanism at loci farther away from core centromeres, whether it sometimes traps individual chromatin fibres and if so whether it is capable of forming chromatin loops. We detected rare instances where the individual DNA trapping occurred on our minichromosomes, namely monomeric DNAs that upon cohesin circularization are retarded in their electrophoretic mobility (form ⑥) in a manner that is destroyed by ring cleavage. Cohesin is known to associate with chromatin prior to DNA replication, when it cannot be involved in holding sisters together. Moreover, it can associate with replicated chromosomes in a manner that does not lead to cohesion between sisters [12,14]. We suggest that cohesin frequently does trap individual chromatin fibres and that its activity in postmitotic cells in metazoan might involve this type of action [15,16]. If we are correct in concluding that cohesin is a novel type of concatenase, then it is not implausible to imagine that other SMC-kleisin complexes such as condensin and its bacterial equivalent have related activities. Indeed, the deep evolutionary roots of these types of complexes suggest that the ability to concatenate DNA may have been an activity without which DNA genomes could not have evolved.

Methods Summary

To establish cysteine cross-linking reactions, the Smc1/Smc3 hinge dimer was co-expressed in *E. coli* and purified via a C-terminal His_6 tag on Smc1 and gelfiltration. The Smc1 head/Scc1-C complex was co-expressed in insect cells using the baculovirus system and purified as described [12]. Proteins were incubated with DMSO, or final concentrations of 200 μM bBBr or 1 mM BMOE before SDS-PAGE and Coomassie staining. Minichromosomes were isolated as described [7] following a slightly modified protocol. Gradient dimer fractions were dialysed against reaction buffer and incubated for 10 minutes with DMSO, 200 μM bBBr, or 1 mM BMOE. Reactions were quenched by addition of DTT to 10 mM and proteins denatured by 4 minutes incubation at 65°C in 1% SDS before agarose gel electrophoresis and Southern blotting. Where indicated, quenched cross-linking reactions were incubated for 1 h at 30°C with TEV protease at 0.2 mg/ml. To measure cross-linking efficiencies in minichromosome fractions, purified protein dimers were added at a final concentration of 3 μM to ensure saturated association of the nanomolar affinity interactions between the dimer subunits.

Acknowledgements

We thank Stephan Gruber for help with the design of cysteine mutations, and Philip Fowler, Dmitri Ivanov,Vito Katis, and all members of the Nasmyth lab for advice and discussions. This work

was supported by the Medical Research Council (MRC), the Wellcome Trust, and Cancer Research UK (CRUK).

References

1. Nasmyth, K. & Haering, C. H. The structure and function of SMC and kleisin complexes. *Annu Rev Biochem* 74, 595-648 (2005).
2. Hirano, T. SMC proteins and chromosome mechanics: from bacteria to humans. *Philosophical transactions of the Royal Society of London* 360 (1455), 507-514 (2005).
3. Uhlmann, F. *et al.* Cleavage of cohesin by the CD clan protease separin triggers anaphase in yeast. *Cell* 103, 375-386 (2000).
4. Haering, C. H., Lowe, J., Hochwagen, A., & Nasmyth, K. Molecular Architecture of SMC Proteins and the Yeast Cohesin Complex. *Mol Cell* 9 (4), 773-788. (2002).
5. Hirano, M. & Hirano, T. Hinge-mediated dimerization of SMC protein is essential for its dynamic interaction with DNA. *EMBO J* 21, 5733-5744 (2002).
6. Gruber, S., Haering, C. H., & Nasmyth, K. Chromosomal cohesin forms a ring. *Cell* 112 (6), 765-777 (2003).
7. Ivanov, D. & Nasmyth, K. A physical assay for sister chromatid cohesion in vitro. *Mol Cell* 27 (2), 300-310 (2007).
8. Milutinovich, M. & Koshland, D. E. Molecular biology. SMC complexes--wrapped up in controversy. *Science* 300 (5622), 1101-1102 (2003).
9. Kim, J. S. & Raines, R. T. Dibromobimane as a fluorescent crosslinking reagent. *Analytical biochemistry* 225 (1), 174-176 (1995).
10. Dhar, G., Sanders, E. R., & Johnson, R. C. Architecture of the hin synaptic complex during recombination: the recombinase subunits translocate with the DNA strands. *Cell* 119 (1), 33-45 (2004).
11. Eswar, N. *et al.* in *Current Protocols in Bioinformatics* (John Wiley & Sons, Inc., 2006), Vol. Supplement 15, 5.6.1-5.6.30, 200.
12. Haering, C. H. *et al.* Structure and stability of cohesin's Smc1-kleisin interaction. *Mol Cell* 15 (6), 951-964 (2004).
13. Gruber, S. *et al.* Evidence that loading of cohesin onto chromosomes involves opening of its SMC hinge. *Cell* 127 (3), 523-537 (2006).
14. Bausch, C. *et al.* Transcription alters chromosomal locations of cohesin in Saccharomyces cerevisiae. *Molecular and cellular biology* 27 (24), 8522-8532 (2007).
15. Schuldiner, O. *et al.* piggyBac-Based Mosaic Screen Identifies a Postmitotic Function for Cohesin in Regulating Developmental Axon Pruning. *Developmental cell* 14 (2), 227-238 (2008).
16. Pauli, A. *et al.* Cell-Type-Specific TEV Protease Cleavage Reveals Cohesin Functions in Drosophila Neurons. *Developmental cell* 14 (2), 239-251 (2008).
17. Megee, P. C. & Koshland, D. A functional assay for centromere-associated sister chromatid cohesion. *Science* 285 (5425), 254-257 (1999).
18. Hwang, D. C. *et al.* Characterization of active-site residues of the NIa protease from tobacco vein mottling virus. *Molecules and cells* 10 (5), 505-511 (2000).

Online Methods

Yeast strains

All strains are derived from W303. Genotypes are listed in Supplementary Table 1.

Model of the *S. cerevisiae* Smc1/Smc3 hinge structure

A structure model of the yeast Smc1/Smc3 hinge structure was created with the Modeller program [11] using an alignment of *S. cerevisiae* Smc1 aa residues 488-690 and Smc3 aa residues 496-699 with aa residues 475-679 of the *T. maritima* SMC protein and the coordinates of pdb file 1GXL.

Expression, purification and cross-linking of cohesin subunit domains

Sequences encoding aa 494-705 of the *S. cerevisiae* Smc3 hinge domain followed by an internal ribosome binding site and sequences encoding aa 486-696 of the *S. cerevisiae* Smc1 hinge domain fused to a C-terminal His_6 tag were cloned by PCR into the pET28 expression vector. Cysteine mutations were introduced by overlap extension PCR. The Smc1/Smc3 hinge domains were co-expressed in *E. coli* strain BL21(DE3)-RIPL (Stratagene) at 20°C for 5 h after induction with 0.25 mM IPTG. Cells were lysed in 50 mM NaP_i pH8.0, 300 mM NaCl containing Complete EDTA free protease inhibitor mix (Roche) and the complex was purified via Ni^{2+}-chelating affinity chromatography followed by gelfiltration on a Superdex 200pg 26/60 column (GE Healthcare) in TEN buffer (20 mM TRIS-HCl pH8.0, 1 mM EDTA, 1 mM NaN_3) +100 mM NaCl +2 mM DTT. The Smc1 head domain bound to Scc1-C was expressed in insect cells using the baculovirus system and purified as described [12].

Purified proteins were re-buffered into reaction buffer (25 mM NaP_i pH7.4, 50 mM NaCl, 10 mM $MgSO_4$, 0.25% Triton X-100) via a Superdex G-25 column, adjusted to 0.5 mg/ml and mixed quickly into $1/25^{th}$ volume of DMSO, 5 mM bBBr (Sigma), or 25 mM BMOE (Pierce). Both cross-linkers were dissolved in DMSO just before use. After 10 min incubation at 4°C, sample loading buffer containing ß-mercaptoethanol was added, the samples were heated for 3 min at 90°C and run on an SDS-PAGE followed by Coomassie blue staining. Cross-linking reached a maximum after a few minutes at 4°C.

Minichromosome preparation and cross-linking

Yeast strains containing the 2.3 kbp minichromosome were grown, arrested in nocodazole and lysed by spheroplasting as described [7], with the exception that sodium citrate and sodium sulfite in the lysis buffer were replaced by 300 mM NaCl to increase minichromosome yield. Extracts were loaded onto an SW41 10-30% sucrose gradient in 25 mM HEPES-KOH pH8.0, 50 mM KCl, 10 mM $MgSO_4$, 0.25% Triton X-100, 1 mM DTT, 1 mM PMSF. Gradients were run for 15 h at 18,000 rpm and fractionated. Fraction aliquots were separated on a 1% agarose gel containing 0.5 µg/ml ethidium bromide as described [7]. Gels were transferred under alkaline conditions by capillary blotting onto Immobilion-NY+ membrane (Millipore). The blots were

hybridized with a ^{32}P-labelled probe for the 2.3 kbp minichromosome sequence, exposed to imaging plates, scanned on an FLA-7000 image analyzer (Fujifilm) and quantified using ImageQuant.

Minichromosome monomer or dimer peak fractions (~300 µl) were dialysed for 4 h against 500 ml reaction buffer at 4°C in a Float-a-lyzer (SpectraPor) with 100 kDa MW cut-off. The dialysis buffer was replaced three times. 24 µl dialysed fraction were mixed quickly into 1 µl DMSO, 5 mM bBBr, or 25 mM BMOE (both freshly dissolved in DMSO) and incubated at 4°C for 10 min. Final concentrations of 200 µM bBBr or 1 mM BMOE were optimal for cross-linking (Supplementary Fig. S7). Bis-malemide based cross-linkers with longer spacers than BMOE, like BMB or BMH (Pierce), could be used with similar efficiency (data not shown). The reaction was quenched by the addition of 1.25 µl 210 mM DTT. For TEV cleavage, 24 µl of the quenched cross-linking reaction was mixed with 1µl 5 mg/ml wild-type or C151A mutant TEV protease in TEV buffer (TEN buffer +50 mM NaCl +2 mM DTT) or TEV buffer only and incubated at 30°C for 1 h. Protein was denatured for 4 min at 65°C after the addition of 2.8 µl 10% SDS. The denatured samples were mixed with 3 µl 80% sucrose containing 0.02% bromophenol blue and 20-25 µl of the mixture were loaded onto a 0.8% agarose gel containing 0.5 µg/ml ethidium bromide. Gels were run at 4°C for 14 h at 1.4 V/cm and blotted and hybridized as before.

For 2D gels, lanes from the first dimension agarose gels were cut out and placed at the top of a second 0.8% agarose gel (20×20 cm) containing 0.5 µg/ml ethidium bromide, leaving an approximately 5 mm wide slot between the lane and the gel. The slot was filled with 60°C warm 0.8% agarose in TAE. Proteinase K was dissolved in TAE and mixed with the pre-warmed agarose solution to a final concentration of 0.2 mg/ml just before casting. Second dimension gels were run at 4°C for 8 h at 2 V/cm, blotted and hybridized as before.

For nicking minichromosome DNA, 200 µl cross-linked samples were first dialysed against 500 ml reaction buffer +2 M KCl +1 mM DTT at 4°C for 4 hours to remove nucleosomes followed by 2 h dialysis against reaction buffer + 1mM DTT to remove salt and 2 h dialysis against reaction buffer +20% sucrose +1 mM DTT to re-concentrate the samples. Dialysis buffers were replaced every hour. 1 µl *Nb.BsrDI* (10 U/µl, NEB) was added to 27 µl sample followed by 10 min incubation at 50°C, addition of SDS to 1% and denaturation as above.

Supplementary Results

Minichromosome cohesion depends on centromeres

To confirm that dimeric minichromosomes detected in sucrose gradients[7] reflect minichromosome cohesion detected *in vivo*[17], we tested whether their generation depends on centromeres. To do this, we created a yeast strain containing a minichromosome whose *CEN4* sequences were flanked by target sites for the site-specific *Zygosaccharomyces rouxii* recombinase (Supplementary Fig. S1a), which was expressed from the galactose-inducible *GAL1* promoter. An exponential culture growing in non-inducing raffinose medium was split and galactose added to one half and glucose to the other. Both sets of cells were arrested in G1 by a factor and then transferred to pheromone-free medium containing nocodazole, which caused them to undergo DNA replication and arrest in a mitotic state. Due to leaky expression of the recombinase, only half of the minichromosomes in glucose grown cells contained *CEN4* prior to DNA replication (Supplementary Fig. S1b). Due to efficient deletion, few if any contained *CEN4* in galactose grown cells.

Minichromosomes containing *CEN4* sequences, either because they contained no recombinase sites or because they had not undergone recombination between them, sediment as dimers and monomers (Supplementary Fig. S1c, top and middle panels). In contrast, minichromosomes whose *CEN4* sequences had been deleted prior to DNA replication sediment almost exclusively as monomers (Supplementary Fig. S1c, lower panel), suggesting that *CEN4* is required for the formation and/or maintenance of minichromosome cohesion. If so, all dimeric minichromosomes from glucose grown cells, which contained equal numbers of intact and deleted minichromosomes, should possess *CEN4* sequences. To test this, monomer and dimer fractions were run on an agarose gel after removal of associated proteins by SDS heat denaturation. This showed that most DNAs migrated as supercoiled circular monomers. Strikingly, almost all DNAs from the dimer fraction had not undergone *CEN4* deletion while most DNAs from the monomer fraction had done so (Supplementary Fig. S1d). We conclude that minichromosomes containing *CEN4* can produce (and maintain) cohesin-mediated dimers during (and after) DNA replication but those lacking *CEN4* cannot.

Calculation of the number of cross-bridges following a Poisson distribution

Following the Poisson distribution, the distribution of x of cross-bridges between minichromosomes will be

$$(1) \quad f(x;\lambda) = \frac{\lambda^x e^{-\lambda}}{x!}$$

$f(0)$ can be determined from the fraction of minichromosomes without cross-bridges ($x = 0$), e.g. the fraction of monomers plus the fraction of dimers that are held together by concatenation (but not by cross-bridges). The percentage of monomers can be directly quantified from gradient blots and is approximately 78% (Supplementary Fig. 4). The fraction of concatemers in the dimer fractions can be directly measured after relaxation of non-crosslinked DNAs with nicking enzyme (Fig. 3d). Alternatively, the ratio of nicked to supercoiled DNA can be measured from monomer fractions (Fig. 4a, panel A, [2]/([1]+[2])). This number can then be used to calculate the proportion of nicked ([2]) and supercoiled-supercoiled concatemers ([3]) in the dimer fractions (Fig. 4a, panel B), yielding the percentage of concatemers (([3]+[4])/total). Using either method, we calculated that 10% of dimers are concatemers. We estimate that approximately 78% + 10%·22% = 80% of minichromosomes are not cohesed, therefore $\lambda = -ln0.8$. The distribution then is

	fraction total circles	**fraction cohesed circles**
$x=0$	$f(0;-ln0.8)=80.0\%$	
$x=1$	$f(1;-ln0.8)=17.8\%$	$f^*(1)=f(1;-ln0.8)/(1-f(0;-ln0.8))=89.3\%$
$x=2$	$f(2;-ln0.8)=2.0\%$	$f^*(2)=f(2;-ln0.8)/(1-f(0;-ln0.8))=10.0\%$
$x=3$	$f(3;-ln0.8)=0.1\%$	$f^*(3)=f(3;-ln0.8)/(1-f(0;-ln0.8))=0.7\%$
	⋮	⋮

We then calculated the fraction of dimers p that are held together by at least one SDS- resistant cross-bridge using the measured crosslinking efficiency $e=30\%$ at both Smc1-Smc3 and Smc1-Scc1 interfaces (Fig. 5c):

	single ring model	**double ring model**
$x=1$	$p(1) = e = 0.30$	$p'(1) = e^2 = 0.09$
$x=2$	$p(2) = 1-(1-e)^2 = 0.51$	$p'(2) = 2e^2 - e^4 = 0.17$
$x=3$	$p(3) = 1-(1-e)^3 = 0.66$	$p'(3) = 3e^2-3e^4+e^6 = 0.25$
	⋮	⋮
	$\Sigma\, p(x)\cdot f^*(x) = \mathbf{0.32}$	$\Sigma\, p'(x)\cdot f^*(x) = \mathbf{0.10}$

In a diploid strain expressing one TEV cleavable and one TEV non-cleavable allele (fraction of non-cleavable molecules $n=50\%$) of the Smc3-Scc1 linker, the fraction of dimers with at least one non-cleaved cross-bridge will be:

	single ring model	**double ring model**
$x=1$	$p''(1) = n = 0.50$	$p'''(1) = n^2 = 0.25$
$x=2$	$p''(2) = 1-(1-n)^2 = 0.75$	$p'''(2) = 2n^2 - n^4 = 0.44$
$x=3$	$p''(3) = 1-(1-n)^3 = 0.88$	$p'''(3) = 3n^2-3n^4+n^6 = 0.58$
	⋮	⋮
	$\Sigma\, p''(x)\cdot f^*(x) = \mathbf{0.53}$	$\Sigma\, p'''(x)\cdot f^*(x) = \mathbf{0.27}$

Supplementary Table

K14856	*MATalpha, smc3::HIS3, smc1::kanMX, scc1::kanMX, leu2::SMC1(G22C, K639C)-myc$_9$::LEU2, ura3::pSCC1-SMC3(E570C)-TEV3-SCC1(A547C)-HA$_6$::URA3, [2.3 kbp TRP1-ARS1-CEN4]*
K14857	*MATa, smc3::HIS3, smc1::kanMX, scc1::kanMX, leu2::SMC1(G22C)-myc$_9$::LEU2, ura3::pSCC1-SMC3-TEV3-SCC1(A547C)-HA$_6$::URA3, [2.3 kbp TRP1-ARS1-CEN4]*
K14858	*MATa, smc3::HIS3, smc1::kanMX, scc1::kanMX, leu2::SMC1-myc$_9$::LEU2, ura3::pSCC1-SMC3-TEV3-SCC1-HA$_6$::URA3, [2.3 kbp TRP1-ARS1-CEN4]*
K14859	*MATalpha, smc3::HIS3, smc1::kanMX, scc1::kanMX, leu2::SMC1(K639C)-myc$_9$::LEU2, ura3::pSCC1-SMC3(E570C)-TEV3-SCC1-HA$_6$::URA3, [2.3 kbp TRP1-ARS1-CEN4]*
K14860	*MATa, scc1::SCC1(TEV3)-HA$_6$::HIS3, [2.3kbp TRP1-ARS1-CEN4]*
K15029	*MATa, top2-4, [2.3 kbp TRP1-ARS1-CEN4]*
K15089	*MATalpha, smc3::HIS3, smc1::kanMX, scc1::kanMX, leu2::SMC1(G22C, K639C)-myc$_9$::LEU2, ura3::pSCC1-SMC3(E570C)-noTEV-SCC1(A547C)-HA$_6$::URA3, [2.3 kbp TRP1-ARS1-CEN4]*
K15249	*MATalpha, smc3::HIS3, scc1::kanMX, smc1::kanMX4, leu2:SMC1-myc$_9$::LEU2, ura3::pSCC1-SMC3(E570C)-TEV3-SCC1(A547C)-HA$_6$::URA3, [2.3 kbp TRP1-ARS1-CEN4]*
K15250	*MATalpha, smc3::HIS3, scc1::kanMX, smc1::kanMX4, leu2:SMC1(K639C)-myc$_9$::LEU2, ura3::pSCC1-SMC3(E570C)-TEV3-SCC1(A547C)-HA$_6$::URA3, [2.3 kbp TRP1-ARS1-CEN4]*
K15251	*MATalpha, smc3::HIS3, smc1::kanMX, scc1::kanMX, leu2::SMC1(G22C, K639C)-myc$_9$::LEU2, ura3::pSCC1-SMC3(E570C)-TEV3-SCC1(A547C)-HA$_6$::URA3, [2.3 kbp TRP1-ARS1-CEN4]*
K15252	*MATa, smc3::HIS3, scc1::kanMX, smc1::kanMX4, leu2::SMC1(G22C)-myc$_9$::LEU2, ura3::pSCC1-SMC3(E570C)-TEV3-SCC1(A547C)-HA$_6$::URA3, [2.3 kbp TRP1-ARS1-CEN4]*
K15301	*MATa, mhra::RS-HMR-E1-RS, leu2::pGAL1-RecR::LEU2 ×2, [2.6 kbp TRP1-ARS1-RS-CEN4-RS]*
K15351	*MATa, leu2::pGAL1-Rec::LEU2, [2.3kbp TRP1-ARS1-CEN4]*
K15267	*MATa/MATalpha, smc3::HIS3/smc3::HIS3, smc1::kanMX4/smc1::kanMX4, scc1::kanMX/scc1::kanMX, leu2::SMC1(G22C, K639C)-myc$_9$::LEU2/leu2::SMC1(G22C, K639C)-myc$_9$::LEU2, ura3::pSCC1-SMC3(E570C)-TEV3-SCC1(A547C)-HA$_6$::URA3/ura3::pSCC1-SMC3(E570C)-noTEV-SCC1(A547C)-HA$_6$::URA3, [2.3 kbp TRP1-ARS1-CEN4]*

Supplementary Table 1 | Yeast strains. All strains are *ade2-1, trp1-1, can1-100, leu2-3,112, his3-11,15, ura3, GAL, psi+* unless noted otherwise.

Supplementary Figures

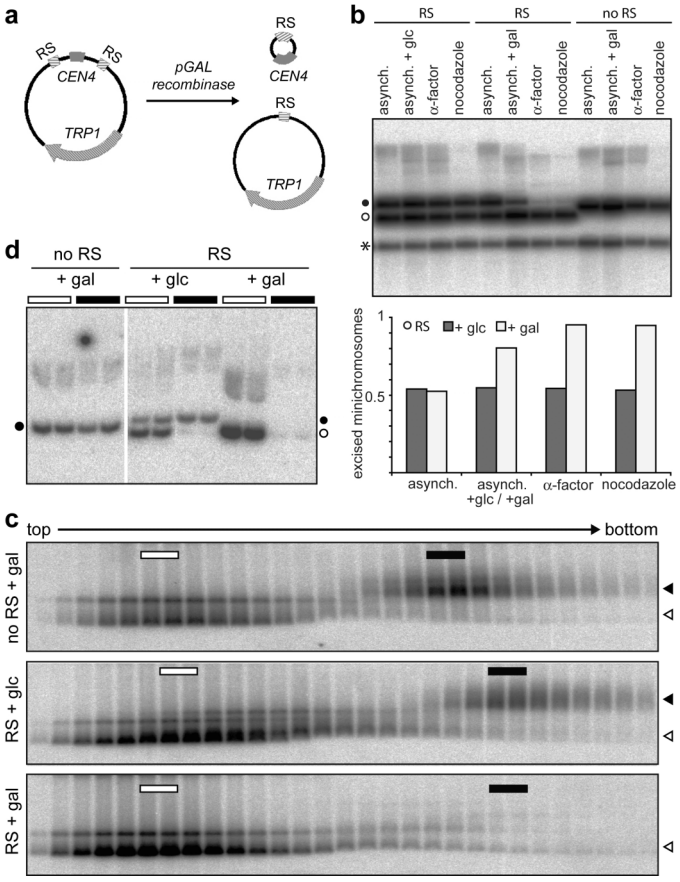

Supplementary Figure S1 | Minichromosome cohesion requires centromeres. a, Induction of *Z. rouxii* recombinase leads to loop-out of the minichromosome centromere region flanked by recombination sites (RS). **b,** Recombinase expression was induced by galactose (+gal) or repressed by glucose (+glc) addition to asynchronous cultures of yeast strains harbouring minichromosomes with centromeres flanked by RS sites (K15301) or without RS sites (K15351) before arresting cells in G1 by α-factor addition. Cells were released from the pheromone arrest into nocodazole containing medium to re-arrest them in a mitotic state. To estimate the efficiency of *CEN4* loop-out, genomic DNA was prepared from asynchronous cultures, 30 min after glucose or galactose addition, or after cells had arrested in α-factor or nocodazole. DNA was linearized with *EcoRI* and probed against the *TRP1* sequence after Southern blotting. Filled circles indicate minichromosomes that still contain *CEN4*, open circles indicates minichromosomes that have looped out *CEN4*. A star marks a restriction fragment of the genomic *TRP1* locus. The fraction of minichromosomes that have excised *CEN4* was quantified and blotted. **c,** Extracts from the nocodazole arrested strains were fractionated by sucrose gradient centrifugation. Gradient fractions were electrophoresed through native agarose gels and minichromosome DNA detected by Southern blotting. Open triangles indicate monomeric and closed triangles indicate dimeric minichromosomes. **d,** DNA from monomer (open bars) and dimer (filled bars) minichromosome gradient fractions were deproteinized by heating for 5 min in 1% SDS, separated by agarose gel electrophoresis, and Southern blotted to measure the fraction of minichromosomes that have looped-out *CEN4*.

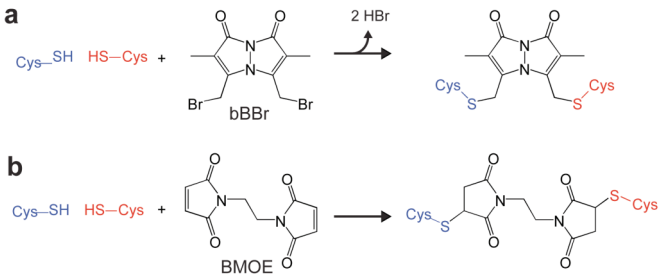

Supplementary Figure S2 | Covalent connection of adjacent cysteine residues. Reaction schemes for crosslinking juxtaposed thiol groups with **a,** dibromobimane (bBBr) and **b,** bis-maleimidoethane (BMOE).

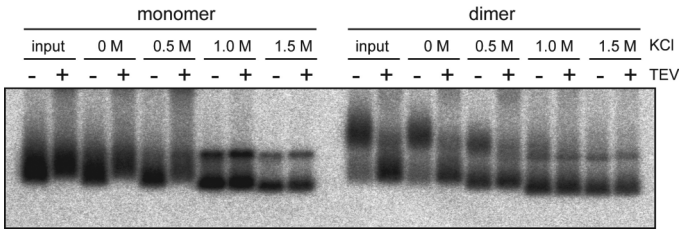

Supplementary Figure S4 | Salt sensitivity of native minichromosome dimers. Minichromosome monomer and dimer gradient fractions from a yeast strain expressing Scc1 with a triple tandem repeat of TEV target sites (K14860) were dialysed for 12 h against reaction buffer containing the indicated concentrations of KCl before removal of high salt by dialysis against reaction buffer without KCl and incubation with TEV protease or buffer only. About 50% of dimers are converted to monomers after incubation with 0.5 M KCl and 100% with 1 M KCl or more.

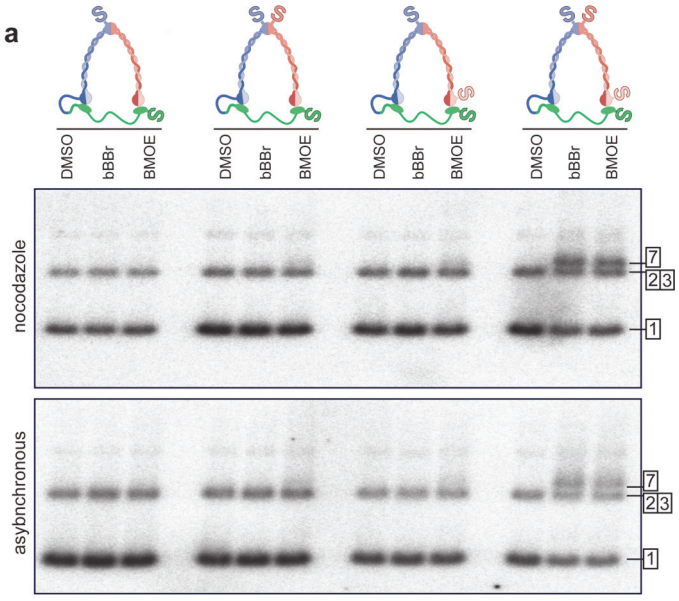

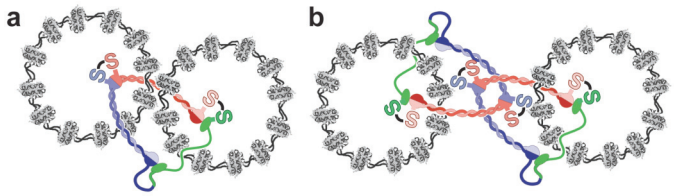

Supplementary Figure S5 | Alternative models for the topological connection of minichromosomes by cohesin rings. a, The single ring model envisions that minichromosomes are held together by their topological entrapment within individual cohesin rings. **b,** The double ring model proposes the entrapment of each minichromosomes within separate cohesin rings that are connected by intertwining.

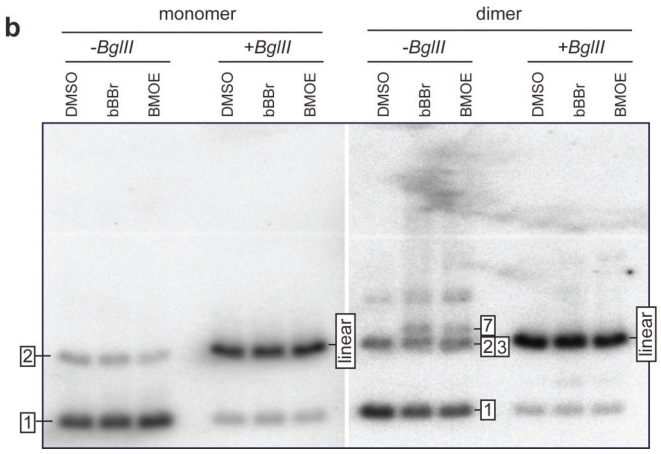

Supplementary Figure S3 | SDS-resistant dimer formation after crosslinking requires all four cysteine substitutions and is lost upon DNA linearization. a, Extracts were prepared from strains expressing the Smc3(E570C)-TEV3-Scc1(A547C) fusion protein containing cysteines in the Smc3 hinge domain the Scc1 C-terminus but lacking both (K15249), either one (K15252, K15250), or none (K15251) of the cysteines in Smc1's hinge and head domains from nocodazole arrested or asynchronous cells and run on sucrose gradients. Dimer fractions were isolated, treated with DMSO, bBBr, or BMOE and analysed by Southern blotting after protein denaturation. Cohesed minichromosome bands ([7]) were only detectable when all four cysteines are present. **b,** Monomer or dimer fractions from a strain (K14856) whose cohesin rings could be covalently circularized were treated with DMSO, bBBr, or BMOE, denatured and run on an agarose gel after incubation with *BglII* restriction enzyme or buffer only. No slower migrating cross-linked dimer bands can be observed after DNA linearization, consistent with the idea that a topological association between circularized cohesin rings and minichromosomes requires intact rings and DNA circles.

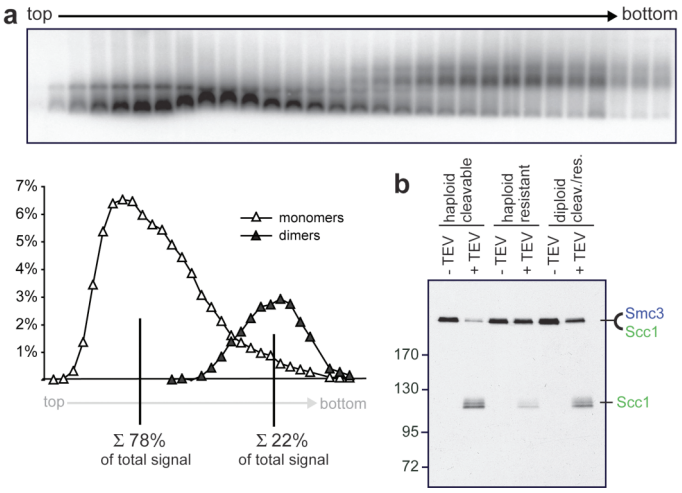

Supplementary Figure S6 | Quantification of minichromosome monomer fraction and Smc3-Scc1 TEV cleavage efficiency. **a,** Gradient fractions from a yeast strain expressing the Smc3-TEV-Scc1 fusion and cysteine pairs at both Smc1/Smc3 and Smc1/Scc1 interfaces (K14856) were run on an agarose gel and Southern blotted. Signal intensities were quantified using a phosphorimager and plotted as percentage of total signal. **b,** Extracts were prepared from haploid strains expressing a single copy of an Smc3-Scc1 fusion protein connected by a TEV-cleavable (K14856) or TEV-resistant (K15089) linker, or from a diploid strain expressing both alleles as single copies (K15267). The fusion proteins were immunoprecipitated via their C-terminal HA_6 tag an the immunoprecipitation beads were incubated with TEV protease or buffer only. The beads were boiled in SDS loading buffer, proteins resolved by SDS-PAGE and the gel was immunoblotted against the HA epitope.

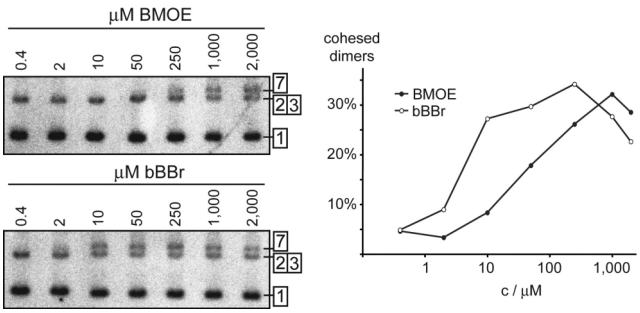

Supplementary Figure S7 | Optimization of cross-linker concentrations. Dimer fractions from a yeast strain expressing the Smc3-TEV-Scc1 fusion and cysteine pairs at both Smc1/Smc3 and Smc1/Scc1 interfaces (K14856) were incubated with increasing concentrations of BMOE (top) or bBBr (bottom) after DTT had been removed by dialysis. The reaction was quenched after 10 min by re-addition of DTT and samples were denatured with 1% SDS, resolved on a 0.8% agarose gel and Southern blotted. Crosslinking efficiencies ([7]/total) are plotted against cross-linker concentration (log-scale). Optimal crosslinking occurred at 1 mM BMOE or 200 µM bBBr.